Advanced Composite Materials
Publication details, including instructions for authors and subscription information:
http://www.tandfonline.com/loi/tacm20

Mechanical Properties of VGCF/MAPP and Atmospheric Plasma-Treated VGCF/PP by Melt-Mixing Process

Nguyen Quang Khuyen [a], Byung Sun Kim [b], Joon Hyung Byun [c] & Soo Lee [d]

[a] Composite Materials Laboratory, Korea Institute of Materials Science (KIMS), 66 Sangnam-dong, Changwon, Gyeongnam, 641-010, Korea

[b] Composite Materials Laboratory, Korea Institute of Materials Science (KIMS), 66 Sangnam-dong, Changwon, Gyeongnam, 641-010, Korea

[c] Composite Materials Laboratory, Korea Institute of Materials Science (KIMS), 66 Sangnam-dong, Changwon, Gyeongnam, 641-010, Korea

[d] Department of Chemical Engineering, Changwon National University, 9 Sarim-dong, Changwon, Gyeongnam, 641-773, Korea

Version of record first published: 02 Apr 2012.

To cite this article: Nguyen Quang Khuyen , Byung Sun Kim , Joon Hyung Byun & Soo Lee (2010): Mechanical Properties of VGCF/MAPP and Atmospheric Plasma-Treated VGCF/PP by Melt-Mixing Process, Advanced Composite Materials, 19:4, 381-392

To link to this article: http://dx.doi.org/10.1163/092430410X504161

///VSP///
Advanced Composite Materials 19 (2010) 381–392
ADVANCED
COMPOSITE
MATERIALS
brill.nl/acm

Mechanical Properties of VGCF/MAPP and Atmospheric Plasma-Treated VGCF/PP by Melt-Mixing Process

Nguyen Quang Khuyen [a,*], **Byung Sun Kim** [a], **Joon Hyung Byun** [a] **and Soo Lee** [b]

[a] Composite Materials Laboratory, Korea Institute of Materials Science (KIMS), 66 Sangnam-dong,
Changwon, Gyeongnam, 641-010, Korea
[b] Department of Chemical Engineering, Changwon National University, 9 Sarim-dong,
Changwon, Gyeongnam, 641-773, Korea

Received 7 January 2009; accepted 22 October 2009

Abstract

The effects of atmospheric plasma treatment and matrix modification by maleic anhydride PP (MAPP) addition, respectively, on the mechanical properties of vapor grown carbon fiber (VGCF)/polypropylene (PP) were investigated. Raw VGCF/PP, raw VGCF/MAPP, atmospheric plasma-treated (APT) VGCF/PP were melt mixed and extruded using a twin-screw extruder. The tensile modulus, shear modulus, and shear strength of APT VGCF/PP showed higher values than those of raw VGCF/PP. The tensile strength, flexural modulus, and flexural strength of raw VGCF/MAPP demonstrated higher values than all the other samples of raw VGCF/PP. The mechanical properties were improved with the atmospheric plasma treatment and coupling agent due to the improved adhesion at VGCF/PP interface. SEM micrographs revealed an excellent dispersion of VGCF in PP and MAPP, respectively. From the twin-screw extruder processing, the VGCF particles were relatively well aligned as well.

Keywords

Polypropylene, maleic anhydride, vapor grown carbon fiber, atmospheric plasma treatment, melt-mixing, interfacial bonding, mechanical properties

1. Introduction

Composites using VGCF are attractive for applications where low density, high strength, and at least moderate conductivity are required, such as electromagnetic interference shielding covers for spacecraft [1]. In particular, it can be expected that, due to the submicron diameters, these fibers could be easily incorporated into the fibrillar structure. When nanocomposites of PP are formed, however, they exhibit significant improvements in physical, chemical and mechanical properties [2, 3].

---

[*] To whom correspondence should be addressed. E-mail: kbs@kims.re.kr
Edited by KSCM

DOI:10.1163/092430410X504161

Usually at very low nanomaterials loading, such nanocomposites exhibit a greatly improved tensile strength, stiffness, better dimensional stability, decreased thermal expansion coefficient, and reduced gas barrier properties in comparison with neat or unfilled polymer resin [3, 4]. In both academic and industrial locations, the study of PP nanocomposites is an area of intense current interest and investigation.

Maleic anhydride (MA) polypropylene has been one of the most suitable coupling agents available for use in fiber-reinforced polypropylene composites [5–7]. A functionalization of the chemically inert surface of the fibers is necessary in order to ensure a good adhesion between the fibers and polymer matrix. Various methods have been reported to modify the surface of carbon fibers, such as chemical treatment [8], thermal treatment [9] and plasma treatment [10, 11]. The atmospheric plasma surface treatment can also assist in creating roughness, area and surface energies to improve the interfacial adhesion between fiber and polymer [10, 11]. The atmospheric surface treatment technology can also be applied for VGCF. The melt-mixing process is the most widespread industrial method. PP and MA together with an initiator are mixed in the molten state at elevated temperatures. The reaction is conducted in an extruder or internal mixer without (or with only a small amount of) solvent in a short processing time. PP powder was mixed with MA and a high concentration of initiator assisted by an interfacial wetting agent [12]. The key points to fully explore VGCF reinforcing potential or enhance the properties of a polymer matrix are uniform dispersion, exfoliation, orientation and improving the interaction between VGCF and PP matrix [13]. In all the cases, the objective was to find the optimum processing method that would utilize carbon fiber's superior properties and lead to nanocomposites with the desired properties.

The aim of the present work is to investigate the mechanical properties of raw VGCF/MAPP and atmospheric plasma-treated VGCF/PP, respectively. It is expected that the atmospheric plasma treatments and coupling agent would enhance the mechanical properties of the resulting VGCF/PP composites. The composite samples were extruded in a cylindrical rod form with 1 mm in diameter. Raw VGCF/PP, raw VGCF/MAPP and APT VGCF/PP were prepared by melt-mixing using a twin-screw extruder.

2. Experimental

2.1. Materials

The VGCFs were from Showa Denko KK. VGCF had specific surface areas of 13 m^2/g, and the diameter and the length were 150 nm and 10–20 μm, respectively. The real density and bulk density of VGCF were 2.0 g/cm^3 and 0.04 g/cm^3, respectively. The aspect ratio (L/D) was 60 with highly crystalline carbon nanofibers synthesized by the gas phase method. They are highly entangled and randomly organized.

A polypropylene powder obtained from Honam Petrochemical Corp. (Korea) was used as a matrix. The specific weight of PP was 0. 95 (g/cm^3), the diame-

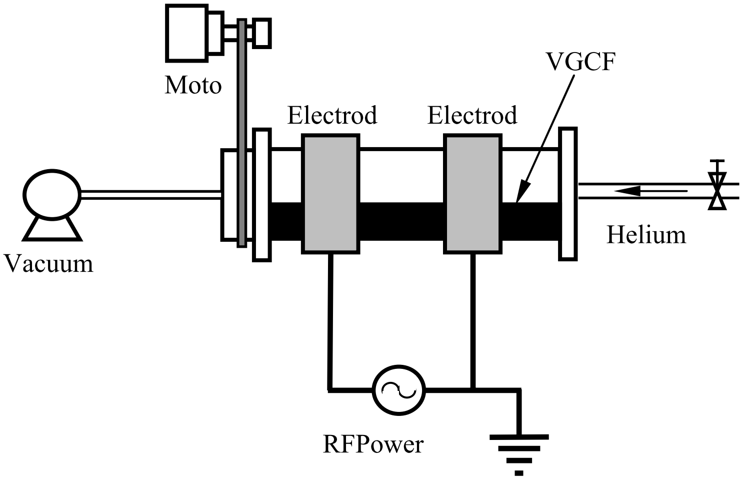

Figure 1. Schematic diagram of the atmospheric plasma treatment process.

ter was 0.5–1.0 mm, the melting point was 170°C, and the molecular weight was 10 000. Using maleic anhydride as a coupling agent (Eastman, USA), the MA has been applied in a 3 wt% to the PP weight. The MA was dispersed in PP matrix by mechanical mixing before the melt-mixing process.

The atmospheric plasma treatment may be used to improve the roughness and surface area of VGCF in order to increase the interfacial bonding between VGCF and PP. APT was created by evacuating a reaction chamber and then refilling it with a low-pressure gas. Using helium as an inert gas, the electrodes were inductively connected around the reactor tube, and the frequency and the voltage were 20 kHz and 3 kV, respectively (Fig. 1).

2.2. *Fabrication of VGCF/PP*

To produce raw VGCF/PP, raw VGCF/MAPP and APT VGCF/PP by melt-mixing process (up to 50 wt%), the VGCFs were sonicated in ethanol for 10 min using the Sonic Mater® sonicator. The solution contained more than 20 ml of ethanol per 1 g of VGCF. The PP powder was then added and mixed under continuous mechanical mixing for an additional hour. The ethanol was dried out and the remaining portion was removed by the vacuum extraction at 80°C for 48 h. The PP powder matrix was melt-mixed by twin-screw extruder (PRIM TSC 16 TC, Thermo Electron Corp.), and then the rod with diameter of 1.0 mm was extruded. The temperatures of five extruder sections from first heating zone to the die were set to 180, 230, 230, 230 and 200°C, respectively. The hopper rate, the screw speed, and the speed of the extruder roll were adequately adjusted for this process. An increase in the temperature of the middle section of the heating zone also helped to decrease the viscosity of VGCF/PP. The weight contents of VGCF were varied from 0.0 to 50.0 wt%. The temperature of the die was set at 250°C with 0.0 to 23.0 wt% of VGCF, and the temperature was decreased to 200°C for 29.0 and 50 wt% of VGCF. As the VGCF

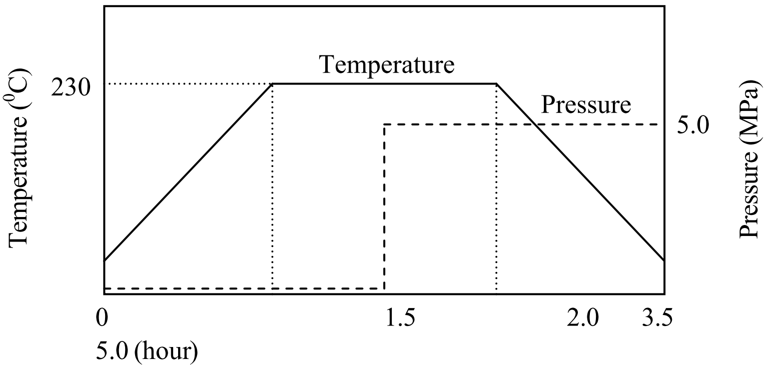

Figure 2. The setting program of temperature and pressure of VGCF/PP.

weight contents increased, the higher temperatures of the die did not result in good rod shape. After extrusion, the VGCF/PP rods were vacuum dried at 90°C for 12 h. The panel was molded in a mold (250 × 80 mm^2). The thickness of the panel of VGCF/PP was controlled by the stopper trip in the mold. The molding condition is shown in Fig. 2. The thicknesses of the molded plates were in a range of 3.0–3.2 mm.

2.3. Mechanical Test

The specimens for tensile, flexural, and shear strength tests were prepared in accordance with ASTM D638 Type IV, ASTM D790M and ASTM D5379, respectively. The tensile and flexural specimen dimensions were 3.0 × 6.0 × 80.0 mm^3 and 3.0 × 12.7 × 60.0 mm^3, respectively. The shear specimen dimensions were 3.0 × 20 × 76 mm^3. Instron 5567 equipment was used for the mechanical test. For the tensile test, the extensometer length was 25.0 mm. The machine was operated under the displacement control mode with speed at 2.00 mm/min. The span used for the flexural test was 40.0 mm, and the speed of the flexural test was 1.00 mm/min. The strain gauges with 5.0 mm lengths were used for the shear sample, and the speed of the shear test was 2.00 mm/min. Five specimens were prepared from each panel for each condition.

2.4. Scanning Electron Microscopy (SEM)

The fracture surfaces of the longitudinal and the transverse directions of raw VGCF/PP, raw VGCF/MAPP and APT VGCF/PP samples were observed by SEM.

2.5. Effect of the Melt-mixing Process on the Dispersion and Arrangement

From continuous melt-mixing process, raw VGCF and APT VGCF were seen to be well-dispersed within PP and MAPP, respectively (Fig. 3).

The ratio of L-tensile strength to T-tensile strength of APT VGCF/PP, and the ratio of L-tensile strength to T-tensile strength of raw VGCF/PP are demonstrated in Fig. 4.

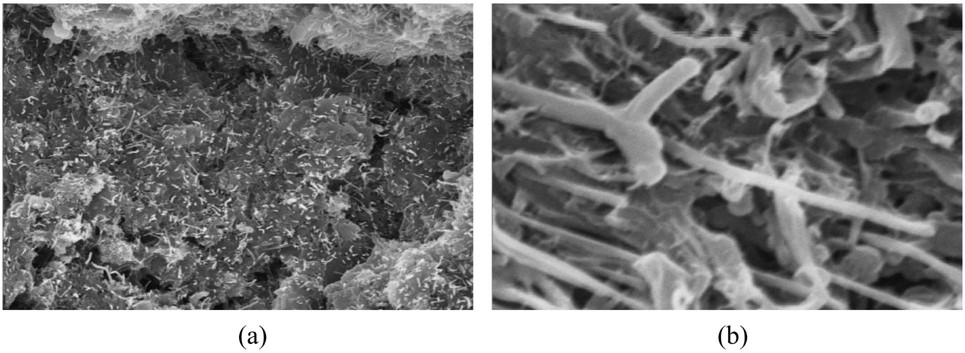
(a) (b)

Figure 3. SEM micrographs revealing the fracture surfaces of (a) longitudinal direction of APT VGCF/PP with 23 wt% VGCF and (b) transverse direction of APT VGCF/PP with 29.0 wt% VGCF.

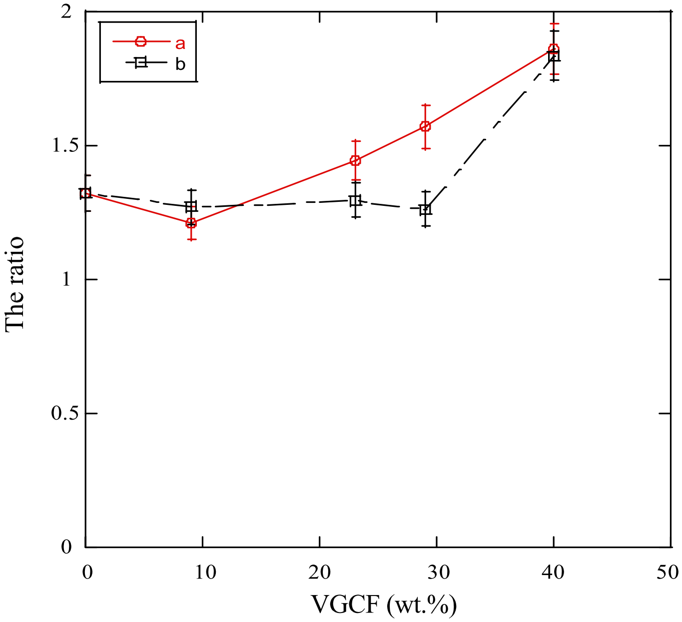

Figure 4. The ratio of L-tensile strength to T-tensile strength of APT VGCF/PP (a) and raw VGCF/PP (b). This figure is published in color on http://www.ingentaconnect.com/content/vsp/acm

During the melt-mixing process, the fibers were strained with the suitable speed of extruder roll in order to improve the VGCF alignments in the PP matrix. The ratio of L-tensile strength to T-tensile strength of APT VGCF/PP increased with increasing nanofiber contents up to 40.0 wt%. Thus, the melt-mixing process with twin-screw extruder provided well-dispersed and improved alignments of VGCF in the PP. The ratio of L-tensile strength to T-tensile strength of APT VGCF/PP showed a higher value than those of raw VGCF with 23.0 and 29.0 wt% VGCF contents, respectively. Hence, the arrangement of APT VGCF in PP matrix was more satisfactory than that of raw VGCF in PP. As a result of TEM, the atmospheric plasma-treated nanofibers were fairly well aligned in PP matrix (Fig. 3(b)).

3. Results and Discussion

3.1. Tensile Properties of Raw VGCF/PP, APT VGCF/PP and Raw VGCF/MAPP

The relationship between tensile modulus of longitudinal direction (L-tensile modulus) and transverse direction (T-tensile modulus) with various VGCF contents are shown in Fig. 5. In order to identify the optimal content of VGCF, the weight fraction of VGCF in PP was varied from 0.0 to 50.0%. The L-tensile modulus and T-tensile modulus of VGCF/PP matrix were increased with increasing VGCF contents up to 50.0 wt%. The L-tensile modulus of raw VGCF/PP was increased by 6.7, 44.3, 46.6, 67.0, 75.9, 86.9 and 117.3% with the addition of 9.0, 17.0, 23.0, 29.0, 33.0, 40.0 and 50.0 wt% of raw VGCF, respectively.

The PP-based nanocomposites containing 29.0 wt% APT VGCF demonstrated the maximum L-tensile modulus values. The L-tensile modulus of APT VGCF/PP with 9.0, 23.0, 29.0 and 40.0 wt% VGCF contents were 127.2, 135.1, 168.8 and 108.1% greater than those of raw VGCF/PP, respectively. The L-tensile modulus

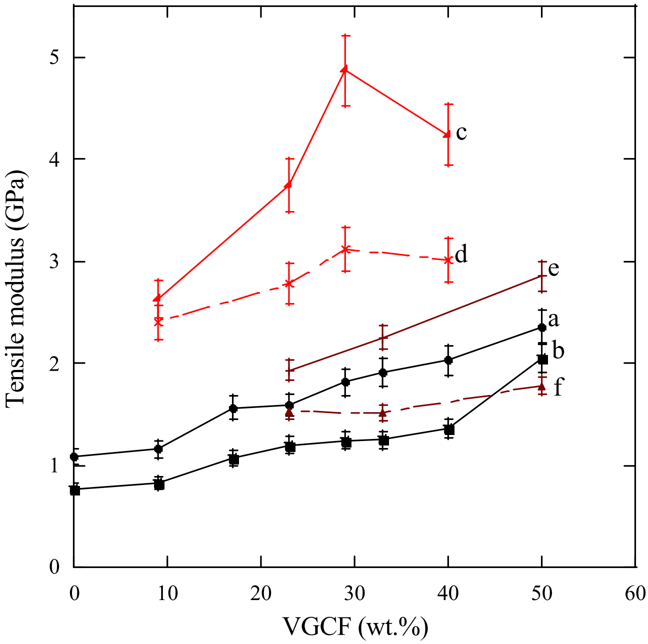

Figure 5. The tensile modulus of raw VGCF/PP, APT VGCF/PP and raw VGCF/MAPP: (a) L-tensile modulus of raw VGCF/PP, (b) T-tensile modulus of raw VGCF/PP, (c) L-tensile modulus of APT VGCF/PP, (d) T-tensile modulus of APT VGCF/PP, (e) L-tensile modulus of raw VGCF/MAPP and (f) T-tensile modulus of raw VGCF/MAPP. This figure is published in color on http://www.ingentaconnect.com/content/vsp/acm

of raw VGCF/MAPP with 23.0, 33.0 and 50.0 wt% VGCF contents were increased by 21.3, 17.9 and 20.9 compared with those of raw VGCF/PP, respectively. The T-tensile modulus of APT VGCF/PP was 190.1, 133.7, 151.0 and 120.8% greater than those of raw VGCF with 9.0, 23.0, 29.0 and 40.0 wt% VGCF contents, respectively. For the raw VGCF/MAPP with 23.0 and 33.0 wt% VGCF contents, the T-tensile modulus were increased by 28.1 and 21.6% compared with those of raw VGCF/PP, respectively. Otherwise, the T-tensile modulus of VGCF/MAPP with 50 wt% of nanofibers was 13.2% lower than that of raw VGCF/PP.

The relationship between tensile strength of the longitudinal direction (L-tensile strength) and transverse direction (T-tensile strength) with various VGCF contents are illustrated in Fig. 6. The L-tensile tensile, T-tensile strength of APT VGCF and raw VGCF/PP matrix showed similar values with varying VGCF contents. The L-tensile strengths of raw VGCF/MAPP were 14.6, 23.5 and 31.6% greater than those of raw VGCF/PP with 23.0, 33.0 and 50.0 wt% VGCF contents, respectively. For 23.0, 33.0 and 50.0 wt% nanofiber contents, the T-tensile strengths of raw VGCF/MAPP were increased by 19.3, 25.5 and 164.7% compared with those of raw VGCF/PP, respectively. The tensile modulus of APT VGCF/PP, and the tensile modulus and strengths of raw VGCF/MAPP showed higher values than those of

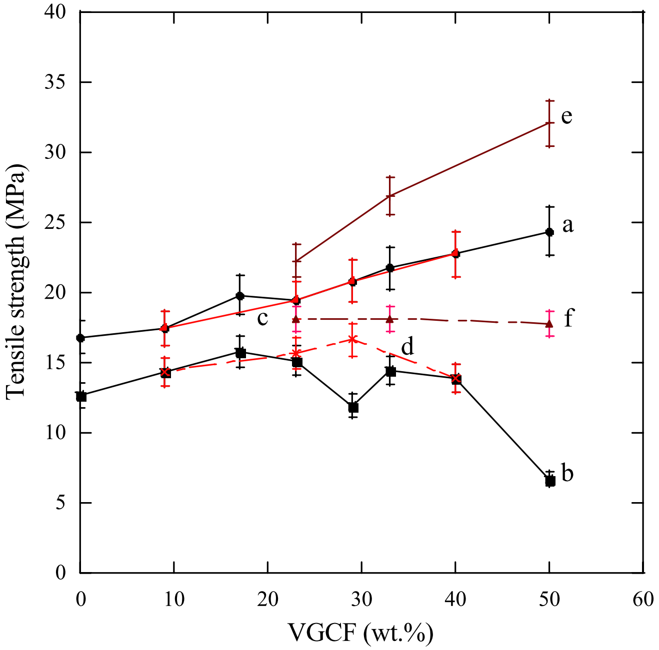

Figure 6. The tensile strength of raw VGCF/PP, APT VGCF/PP and raw VGCF/MAPP: (a) L-tensile strength of raw VGCF/PP, (b) T-tensile strength of raw VGCF/PP, (c) L-tensile strength of APT VGCF/PP, (d) T-tensile strength of APT VGCF/PP, (e) L-tensile strength of raw VGCF/MAPP and (f) T-tensile strength of raw VGCF/MAPP. This figure is published in color on http://www.ingentaconnect.com/content/vsp/acm

raw VGCF/PP in all VGCF contents. Thus, the atmospheric plasma treatment and coupling agent had strongly affected the tensile modulus and strengths of VGCF/PP.

3.2. Flexural Properties of Raw VGCF/PP, APT VGCF/PP and Raw VGCF/MAPP

The relationship between the flexural modulus of longitudinal direction (L-flexural modulus) and transverse direction (T-flexural modulus) with various VGCF contents are showed in Fig. 7. It can be observed that the VGCF provides a significant reinforcing effect with the PP matrix. After the addition of the fillers, the flexural modulus of the VGCF/PP matrix was noticeably improved. The flexural modulus of VGCF/PP matrix was increased with increasing VGCF contents. Enhancements of 26.1, 55.2, 80.6, 107.1, 114.3, 143.6 and 201.6% in L-flexural modulus for the PP matrix were obtained after adding 9.0, 17.0, 23.0, 29.0, 33.0, 40.0 and 50.0 wt% raw VGCF, respectively.

The L-flexural modulus, T-flexural modulus of APT VGCF and the raw VGCF/PP had similar values with the same VGCF contents. Thus, the atmospheric plasma treatments have no effect on the flexural modulus. Indeed, the VGCF is such a short fiber that the interfacial bonding between the short fiber and poly-

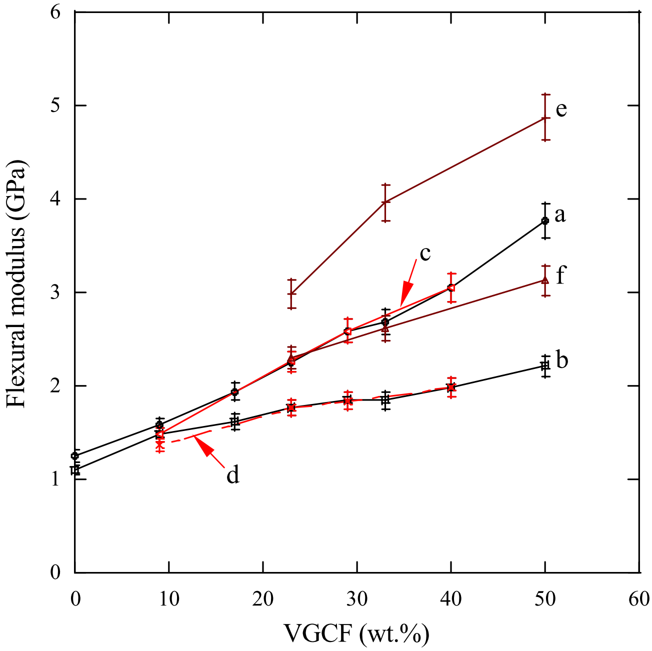

Figure 7. The flexural modulus of raw VGCF/PP, APT VGCF/PP and raw VGCF/MAPP: (a) L-flexural modulus of raw VGCF/PP, (b) T-flexural modulus of raw VGCF/PP, (c) L-flexural modulus of APT VGCF/PP, (d) T-flexural modulus of APT VGCF/PP, (e) L-flexural modulus of raw VGCF/MAPP and (f) T-flexural modulus of raw VGCF/MAPP. This figure is published in color on http://www.ingentaconnect.com/content/vsp/acm

mer matrix has no effects on the flexural modulus. The surface area of VGCF was increased after plasma treatment, without further influence on flexural modulus. Using maleic anhydride (MA) as a coupling agent, the MA functional group grafted onto the end of long PP chains. Thus, the PP matrix increased the stiffness, and the MAPP-modified hybrid composites showed higher flexural modulus than unmodified hybrid composite ones [9]. According to our results, the L-flexural modulus of 23.0, 33.0 and 50.0 wt% raw VGCF/MAPP were 32.4, 47.8 and 29.1% greater than those of raw VGCF/PP, respectively. The T-flexural strengths of raw VGCF/MAPP were increased by 30.0, 41.7 and 29.2% compared with those of raw VGCF/PP with 23.0, 33.0 and 50.0 wt% VGCF contents, respectively.

The relationship between the flexural strength of longitudinal direction (L-flexural strength) and transverse direction (T-flexural strength) are presented in Fig. 8. The T-flexural strength of raw VGCF/PP matrix was increased with increasing VGCF contents. The enhancements in T-flexural flexural obtained with VGCF implied that carbon nanofibers are a very promising candidate to be used as reinforcement for PP-nanocomposites. When compared to raw VGCF/PP, the L-flexural strengths of raw VGCF/MAPP were increased by 22.1, 27.4 and 19.7% with 23.0, 33.0 and 50.0 wt% VGCF contents, respectively. The T-flexural strengths of raw

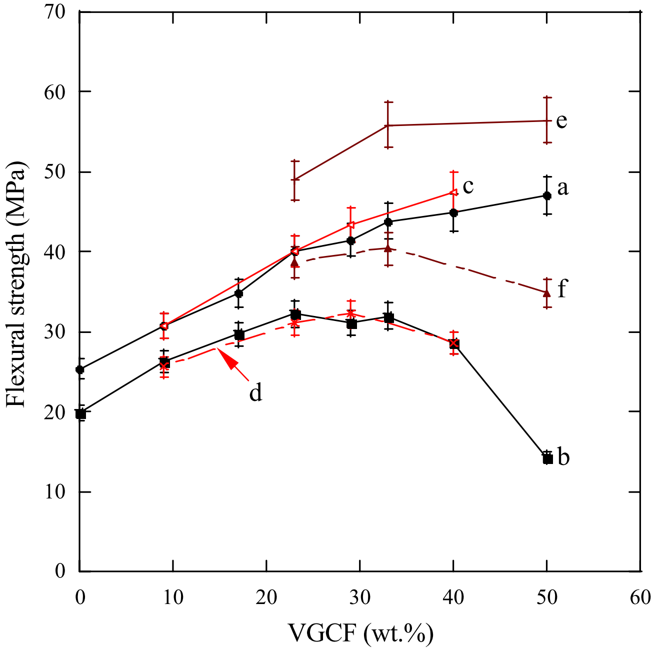

Figure 8. The flexural strength of raw VGCF/PP, APT VGCF/PP and raw VGCF/MAPP: (a) L-flexural strength of raw VGCF/PP, (b) T-flexural strength of raw VGCF/PP, (c) L-flexural strength of APT VGCF/PP, (d) T-flexural strength of APT VGCF/PP, (e) L-flexural strength of raw VGCF/MAPP and (f) T-flexural strength of raw VGCF/MAPP. This figure is published in color on http://www.ingentaconnect.com/content/vsp/acm

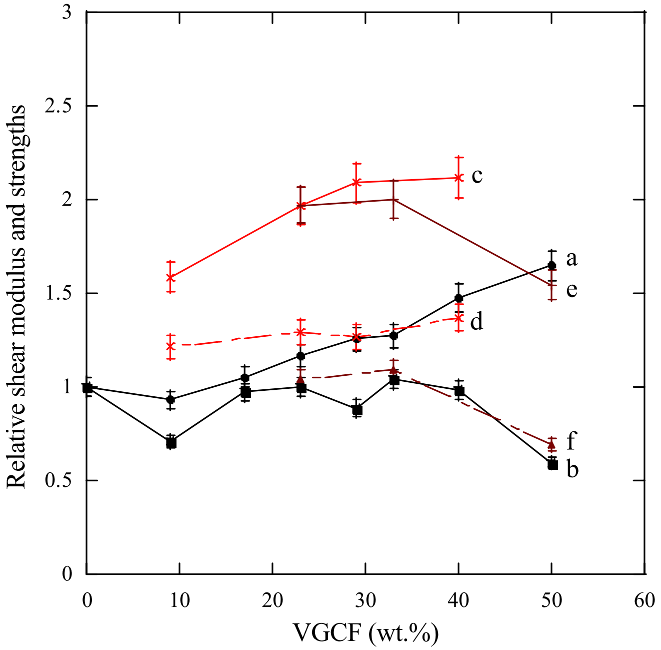

Figure 9. The relative T-shear modulus and relative T-shear strength of raw VGCF/PP, APT VGCF/PP and raw VGCF/MAPP: (a) T-shear modulus of raw VGCF/PP, (b) T-shear strength of raw VGCF/PP, (c) T-shear modulus of APT VGCF/PP, (d) T-shear strength of APT VGCF/PP, (e) T-shear modulus of raw VGCF/MAPP and (f) T-shear strength of raw VGCF/MAPP. This figure is published in color on http://www.ingentaconnect.com/content/vsp/acm

VGCF/MAPP were 20.3, 26.2 and 144.1% greater than those of raw VGCF/PP with 23.0, 33.0 and 50.0 wt% nanofibers contents, respectively. Accordingly, the cross-linking network in the raw VGCF/MAPP has improved.

3.3. Shear Properties of Raw VGCF/PP, APT VGCF/PP and Raw VGCF/MAPP

The shear modulus in transverse direction (T-shear modulus) and the shear strength in transverse direction (T-shear strength) with various VGCF contents are shown in Fig. 9. The T-shear modulus of raw VGCF/PP matrix was increased with increasing VGCF contents up to 50.0 wt%. The T-shear modulus of APT VGCF/PP with 9.0, 23.0, 29.0 and 40.0 wt% VGCF contents was increased by 70.0, 68.4, 66.3 and 43.4% compared with those of raw VGCF/PP, respectively. For the raw VGCF/MAPP, the T-shear modulus of PP-nanocomposites with 23.0, 33.0 and 50.0 wt% VGCF contents were 68.9 and 57.2% greater, and 5% smaller than those of raw VGCF/PP, respectively. The optimal VGCF content for APT VGCF/PP was found to be 40.0 wt%.

The ratio of T-shear strength of APT VGCF/PP and T-shear strength of raw VGCF/PP were 1.71, 1.29, 1.43 and 1.39 with 9.0, 23.0, 29.0 and 40.0 wt% VGCF contents, respectively. The T-shear strengths of raw VGCF/MAPP and raw

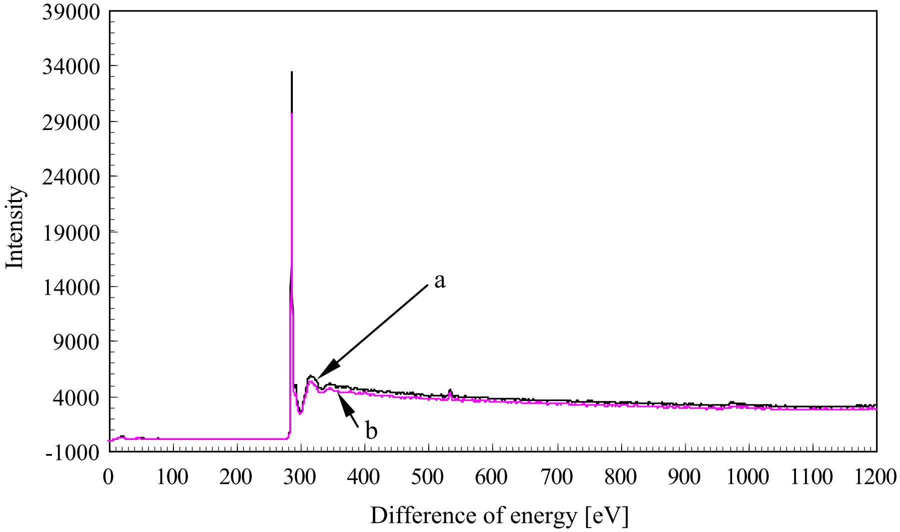

Figure 10. XPS spectra of (a) raw VGCF and (b) APT VGCF. This figure is published in color on http://www.ingentaconnect.com/content/vsp/acm

VGCF/PP had similar values. Thus, the atmospheric plasma treatment had affected the interfacial bonding between VGCF and PP, while the coupling agent did not have an influence on the T-shear strength of VGCF/PP.

X-ray photoelectron spectroscopy (XPS) results for the VGCF also showed that there was no chemical function on the surface of nanofibers after by atmospheric plasma treatment (Fig. 10).

4. Conclusions

Atmospheric plasma treatments were conducted with helium to modify the surface properties of VGCF and using maleic anhydride as a coupling agent in order to improve the interfacial bonding between the VGCF and PP matrix. Raw VGCF and APT VGCF were dispersed uniformly throughout the PP and MAPP matrix by means of melt blending with a twin-screw extruder. The effects of atmospheric plasma treatments and coupling agent on the mechanical properties of VGCF/PP composites were discussed.

The mechanical properties of raw VGCF/MAPP and APT VGCF/PP were compared with those of raw VGCF/PP. The atmospheric plasma treatment and coupling agent affected mechanical properties of VGCF/PP nanocomposites. The tensile modulus, shear modulus and shear strength of APT VGCF/PP were higher than those of raw VGCF/PP. The tensile modulus, tensile strength, flexural modulus, flexural strength and shear modulus of raw VGCF/MAPP were greater than those of raw VGCF/PP. The twin-screw extruder process allowed good dispersion and improved the alignment of VGCFs in PP.

Acknowledgement

This work was supported by the Korea Foundation for International Cooperation of Science and Technology (KICOS) through a grant provided by the Korea Ministry of Education, Science and Technology (MEST) in 2007 (No. 20704000090).

References

1. M. M. Hasan, Y. Zhou and S. Jeelani, Thermal and tensile properties of aligned carbon nanofiber reinforced polypropylene, *Mater. Letts* **61**, 1134–1136 (2007).
2. D. Bikiaris, A. Jannakoudakis and A. Docoslis, Effect of acid treated multi-walled carbon nanotubes on the mechanical, permeability, thermal properties and thermo-oxidative stability of isotactic polypropylene, *Polym. Degrad. Stabil.* **93**, 952–967 (2008).
3. A. Funck and W. Kaminsky, Polypropylene carbon nanotube composites by *in situ* polymerization, *Compos. Sci. Technol.* **67**, 906–915 (2007).
4. S. A. Gordeyev, J. A. Ferreira, C. A. Bernardo and I. M. Ward, A promising conductive material: highly oriented polypropylene filled with short vapour-grown carbon fibres, *Mater. Letts* **51**, 32–36 (2001).
5. G. W. Beckermann and K. L. Pickering, Engineering and evaluation of hemp fibre reinforced polypropylene composites: fibre treatment and matrix modification, *Composites: Part A* **39**, 979–988 (2008).
6. J. Z. Lu, Q. Wu and H. S. M. Nabb, Chemical coupling in wood fiber and polymer composites: a review of coupling agents and treatments, *Wood Fiber Sci.* **32**, 88–104 (2000).
7. A. Arbelaiz, B. Fernández, G. Cantero, R. Llano-Ponte, A. Valea and I. Mondragon, Mechanical properties of flax fibre/polypropylene composites. Influence of fibre/matrix modification and glass fibre hybridization, *Composites: Part A* **36**, 1637–1644 (2005).
8. K. K. C. Ho, A. F. Lee and A. Bismarck, Fluorination of carbon fibres in atmospheric plasma, *Carbon* **45**, 775–784 (2007).
9. S. Lee, S. Y. Da, A. A. Ogale and M. S. Kim, Effect of heat treatment of carbon nanofibers on polypropylene nanocomposites, *J. Phys. Chem. Solids* **69**, 1407–1410 (2008).
10. S. J. Park and H. Y. Lee, Effect of atmospheric-pressure plasma on adhesion characteristics of polyimide film, *J. Coll. Interf. Sci.* **285**, 267–272 (2005).
11. Y. Kusano, H. Mortensen, B. Stenum, S. Goutianos, S. Mitra, A. Ghanbari-Siahkali, P. Kingshott, B. F. Sørensen and H. Bindslev, Atmospheric pressure plasma treatment of glassy carbon for adhesion improvement, *Intl J. Adhes. Adhes.* **27**, 402–408 (2007).
12. W. Qiu, T. Endo and T. Hirotsu, A novel technique for preparing of maleic anhydride grafted polyolefins, *Eur. Polym. J.* **41**, 1979–1984 (2005).
13. F. Rezaei, R. Yunus and N. A. Ibrahim, Effect of fiber length on thermomechanical properties of short carbon fiber reinforced polypropylene composites, *Mater. Design* **30**, 260–263 (2009).